

Supporting Information

New Chemical Reaction Process of a $\text{Bi}_2\text{Te}_{2.7}\text{Se}_{0.3}$ Nanomaterial for Feasible Optimization in Transport Properties Resulting in Predominant n-type Thermoelectric Performance

Cham Kim^{1,*}, Chang Eun Kim¹, Ju Young Baek¹, Dong Hwan Kim¹, Jong Tae Kim¹, Ji Hyeon Ahn¹,
David Humberto Lopez², Taewook Kim³, Hoyoung Kim¹

¹ Daegu Gyeongbuk Institute of Science and Technology (DGIST), 333 Techno Jungang-daero, Daegu,
42988, Republic of Korea

² Department of Chemical and Environmental Engineering, University of Arizona, 1133 E. James. E.
Rogers Way, Tucson, AZ, 85721, USA

³ Department of Chemical Engineering, Pohang University of Science and Technology (POSTECH), 77
Cheongam-Ro, Pohang, 37673, Republic of Korea

*Corresponding author. E-mail: charming0207@dgist.ac.kr (C. Kim);

Tel.: +82-53-785-3602; fax: +82-53-785-3609.

Table S1. Atomic composition ratios of the ternary products obtained in the chemical reaction process measured using ICP-MS. The bismuth ratios were chosen as reference points.

No.	Bi			Te			Se		
	Concentration		At. ratio	Concentration		At. ratio	Concentration		At. ratio
	mg L ⁻¹	mmol L ⁻¹		mg L ⁻¹	mmol L ⁻¹		mg L ⁻¹	mmol L ⁻¹	
1	460.6	2.204	2.00	380.2	2.980	2.70	26.72	0.338	0.31
2	498.2	2.384	2.00	416.9	3.267	2.74	27.54	0.349	0.29
3	492.3	2.356	2.00	409.0	3.205	2.72	28.06	0.355	0.30
Ave.	483.7	2.315	2.00	402.03	3.151	2.72	27.44	0.348	0.30

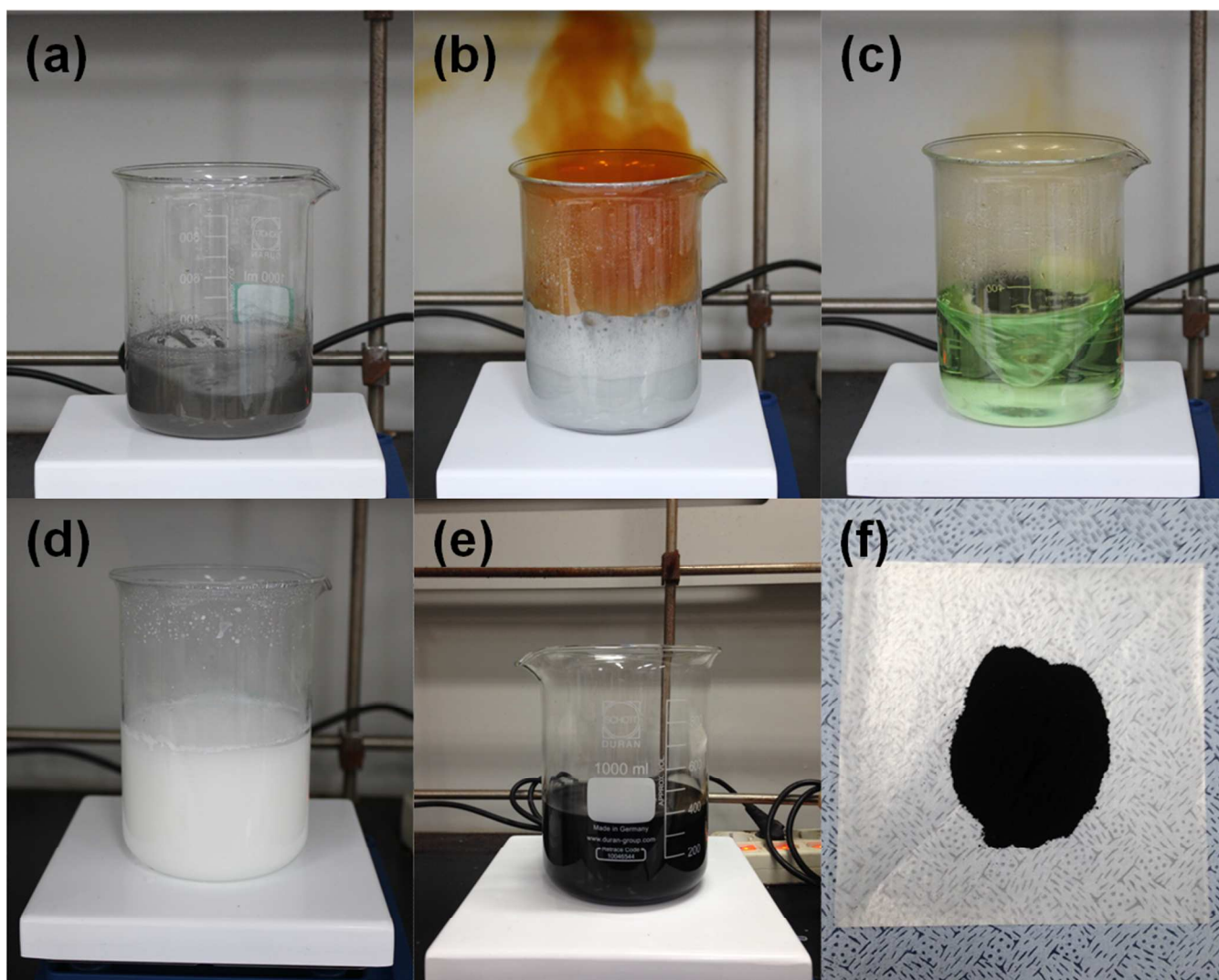


Figure S1. Chemical reaction process for synthesizing Bi_2Te_3 -based nanocrystalline materials: (a) tellurium powders initially soaked in aqueous nitric acid solution, (b) tellurium oxidation in the nitric acid solution, (c) simultaneous oxidation of bismuth and tellurium, (d) co-precipitation of the oxidized species, (e) reduction of the precipitate, and (f) the reduced powder obtained by washing and drying.

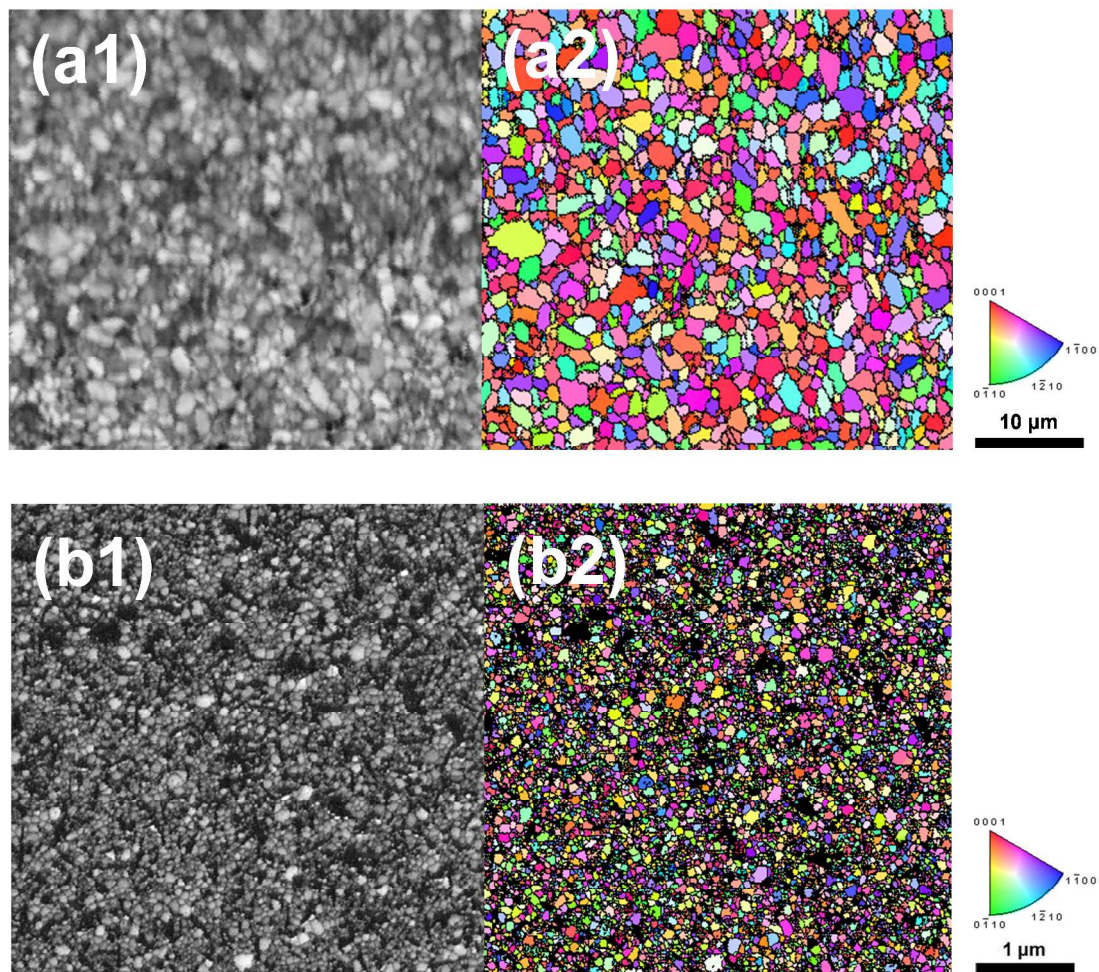


Figure S2. Electron backscatter diffraction (EBSD) images of specimens sintered from the $\text{Bi}_2\text{Te}_{2.7}\text{Se}_{0.3}$ prepared via the ionic reaction in the previous work¹ (a) and the $\text{Bi}_2\text{Te}_{2.7}\text{Se}_{0.3}$ synthesized in the present study (b). The EBSD images are provided as an image-quality map (1) and an inverse pole figure (2) for each specimen.

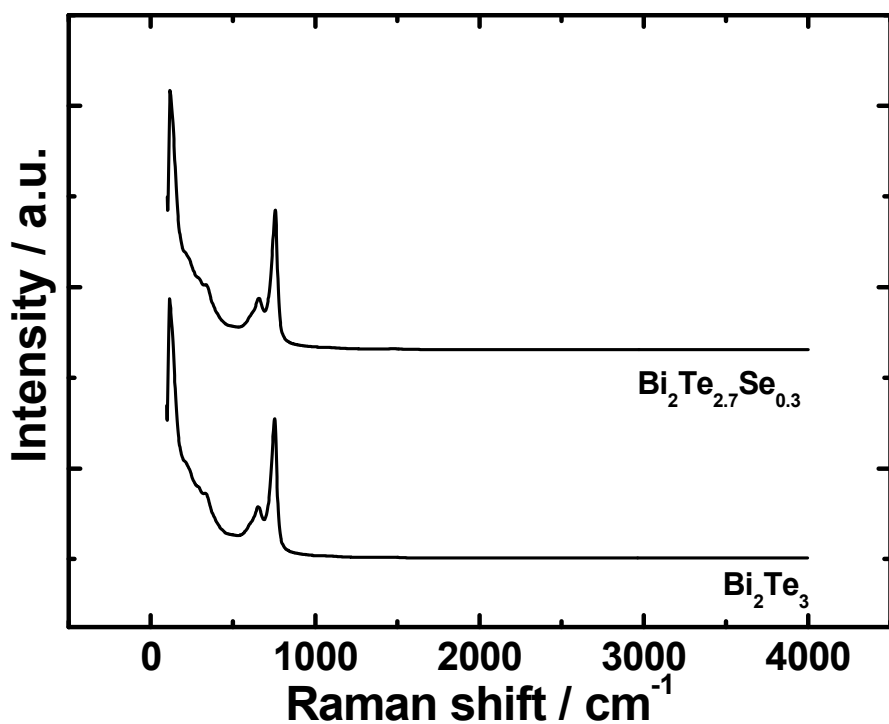


Figure S3. Raman spectra of the $\text{Bi}_2\text{Te}_{2.7}\text{Se}_{0.3}$ and Bi_2Te_3 nanocompounds in the frequency region ranging from 100 to 4000 cm^{-1} . The spectra exhibit the Raman and IR active vibrational modes of rhombohedral Bi_2Te_3 in the low frequency region below 200 cm^{-1} as presented in detail in Figure 1b, while they show distinct peaks in the higher region (from 500 to 1,000 cm^{-1}), indicative of the overtone modes that possibly arise due to defect-induced symmetry breaking.²⁻⁴

References

- (1) Kim, C.; Kim, D. H.; Kim, J. T.; Han, Y. S.; Kim, H. Investigation of Reaction Mechanisms of Bismuth Tellurium Selenide Nanomaterials for Simple Reaction Manipulation Causing Effective Adjustment of Thermoelectric Properties. *ACS Appl. Mater. Interfaces* **2014**, *6*, 778–785.
- (2) Puneet, P.; Podila, R.; Karakaya, M.; Zhu, S.; He, J.; Tritt, T. M.; Dresselhaus, M. S.; Rao, A. M. Preferential Scattering by Interfacial Charged Defects for Enhanced Thermoelectric Performance in Few-layered *n*-type Bi₂Te₃. *Sci. Rep.* **2013**, DOI:10.1038/srep03212.
- (3) Russo, V.; Bailini, A.; Zamboni, M.; Passoni, M.; Conti, C.; Casari, C. S.; Bassi, A. L.; Bottani, C. E. Raman Spectroscopy of Bi-Te Thin Films. *J. Raman Spectrosc.* **2008**, *39*, 205–210.
- (4) Zheng, Z. H.; Fan, P.; Chen, T. B.; Cai, Z. K.; Liu, P. J.; Liang, G. X.; Zhang, D. P.; Cai, X. M. Optimization in Fabricating Bismuth Telluride Thin Films by Ion Beam Sputtering Deposition. *Thin Solid Films* **2012**, *520*, 5245–5248.